Stochastic Scheduling of Primary Frequency Response for Uncertain Low Carbon Power System

Vivek Prakash,Rohit Bhakar, Harpal Tiwari,
Department of Electrical Engineering, Malaviya National Institute of Technology Jaipur, India
Email: vivekprakashee@gmail.com, rohitbhakar@gmail.com, harpaltiwari@yahoo.co.in

***Abstract*— Strong government policy targets to achieve large generation from uncertain renewable energy sources (RES) like wind and PV generation is likely to pose real-time operational challenges for the utilities to provide primary frequency response (PFR). PFR requirement for fast frequency stability following a largest generation outage has been known widely and its scheduling needs wider investigation. This necessitates optimized PFR scheduling from generation scheduling and quantification of associated uncertainty. In this perspective, this paper proposes a novel stochastic scheduling model for operation and PFR cost minimization, with optimized PFR schedules under wind and PV generation uncertainty. Case studies are carried out on one area IEEE RTS and the proposed method is compared with the conventional deterministic unit commitment (DUC). Numerical results show the ability of the proposed method in terms of optimized PFR schedules, reduction in operation cost, PFR cost and has potential to provide solutions for enhanced fast frequency control for low carbon power systems.**

Keywords- Inertia; stochastic scheduling; primary frequency response; PV; uncertainty, wind.

I. INTRODUCTION

Global requirement of green and clean energy with low carbon emission necessitates, RES to meet the ever increasing demand of energy. Among the variety of RES, wind and solar power are contributing the largest proportion with approximately 400 GW of wind and 200 GW of solar been installed world-wide in the 2016 [1],[2]. Larger integration of RES in to the grid will displace the conventional generation at a fast rate. Displacement of synchronous generation with these intermittent generation sources is likely to create several operational challenges for the grid operators, such as system inertia reduction, weakening of system strength, increase in distributed generation and the prospect of advance technologies interface with the grid pose range of operational challenges [3],[4].

Generation characteristics of wind and PV are different from those of conventional generation. Uncertainties, such as wind speed, cloud transients, solar insolation, increase the operational risk and affect generator output continuously. Normally, RES are installed with frequency relay that isolates after a frequency disturbance. When there is large RES penetration in the grid, a massive RES disconnection could lead to power system instability. As RES penetration increases, the fluctuations of generated power increases whilst overall system inertia is reduced [5]. There is a reduction in the frequency nadir and settling frequency because of the lack of inertial response and PFR from RES and the displacement of responsive conventional generation.

Recent analysis in National Grid (United Kingdom) finds that frequency response requirements would increase significantly over the next 15 years [6]. PFR requirement amounts to an increase of 30-40% over the next five years. This necessitates a wider understanding of the research opportunities & challenges arising out of large penetration of renewables in the grid and how evolving system technologies and modelling could be used to create opportunities for reliable and secure system operation.

PFR constraints have been modeled, explicitly covering only steady state frequency deviation and governor droop to determine if sufficient primary reserves are committed [7]. However, transient frequency behavior and frequency droop parameter for unit regulation have not been considered. This assessment is considered in SUC model; PFR and steady state frequency response with uncertainties like generation outage, wind generation and demand are included. The response delivery time of all generators has been assumed identical [8]. However, these assumptions may not provide the exact deployment time of the PFR. PFR deployment time constraint is included in stochastic and security constrained generation scheduling model which include fast frequency response constraints while considering wind generation uncertainty [9]. However, PFR scheduling with wind and PV generation uncertainty has not been fully envisaged.

In this context main contribution of this paper could be summarized as follows:

(i) It proposes a novel stochastic scheduling formulation concept that includes system's fast frequency response constraints that directly aims to contain the initial transient frequency behavior within the prescribed system security criteria like ROCOF, frequency nadir and intermediate state of frequency following a largest infeed loss.

(ii) It provides PFR schedules of committed generators following a large infeed loss.

(iii) It characterizes the wind and PV power uncertainty for the proposed stochastic scheduling formulation using ARIMA model, which is one of the most popular approach for modelling any stochastic process; with the aim to improve the day-ahead unit scheduling procedures and optimal PFR schedules. Uncertainty is modelled using scenario generation and reduction technique.

This work is supported by the DST grant for HEAPD project, DST/RCUK/SEGES/2012/09.

(iv) It demonstrates the efficacy of the proposed model on one area IEEE RTS system through systematic comparative assessment with deterministic UC, for their PFR scheduling performance; & Cost performance with varying wind penetration.

II. PFR REQUIREMENT

The objective of PFR control is to arrest initial frequency deviation within the prescribed network security criteria at the transient conditions. Security criteria that effect PFR characteristics are rate of change of frequency (RoCoF), frequency nadir, f^{nadir} and intermediate steady-state frequency, f^{ss} as shown in Fig. 1. [10]. The RoCoF depends on the synchronized inertial response and the capacity of generation outage.

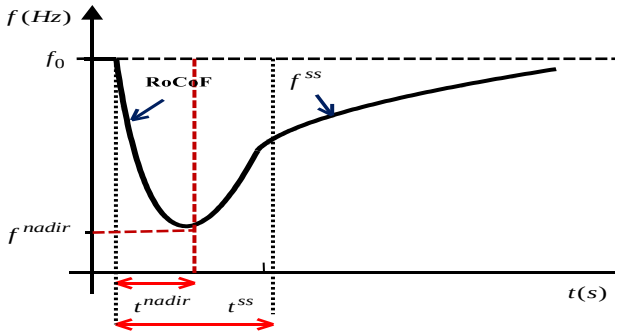

Fig.1. Frequency response characteristics after sudden infeed loss

The rise in RoCoF slope can actuate generator protection settings and lead to demand disconnection. Therefore, PFR should restrict the frequency above f^{nadir} and stabilize above f^{ss}. Full PFR is required to deliver between 10 and 30 s. This would depend on the droop constant setting, dead-band, available headroom and load damping rate.

III. STOCHASTIC SCHEDULING MODEL

The problem objective is to minimize the expected operating cost. The basic scheduling formulation has been modified to incorporate frequency response constraints requirements [11]. It considers the cost of each scenario in proportion to its probability. The objective function includes no-load cost, start-up cost and operating cost of all the generators, along with the cost of enabling the governor and lost load cost as shown by Eqn. (1).

$$\min \sum_{t\in T}\sum_{i\in I}(A_i.x_{i,t} + su_{i,t} + LS_t * VOLL + \delta_{i,t}.C_i^{ge} + \sum_{n\in N}\pi_n \sum_{b\in B} K_{i,b}.g_{i,t,b,n}) \quad (1)$$

Where, I, T, N, B, S, J and G_{ng} are the set of generators, time interval, scenarios, buses and linear segment of cost curve, generator start-up cost and generators without enabled governor respectively, while i, t, n, b, s, j are the index of generators, time intervals, scenarios, buses and each generator cost curve, start-up cost, respectively. A_i is no-load cost of generator i ($), $x_{i,t}$ is the generator on/off status variable, $su_{i,t}$ is the variable for start-up cost of generator i during hour t ($), LS_t is denoting the load shedding variable at time interval t (MW), $VOLL$ is the value of loss load ($/MW-h), $\delta_{i,t}$ is the variable for generator governor enabled while c_i^{ge} is the cost of enabling the governor($), π_n is the probability of scenario n, $K_{i,s}$ is the S^{th} segment slope of the generator i cost curve ($/MW) and $g_{i,t,s,n}^{seg}$ is the power output of generator i on segment s under scenario n during hour t.

The optimization problem is subject to following operational constraints.

$$y_{i,t} - z_{i,t} = x_{i,t} - x_{t-1,i}, \quad \forall t \in T, i \in I \quad (2)$$

$$y_{i,t} + z_{i,t} \le 1, \quad \forall t \in T, i \in I \quad (3)$$

Constraint (2) determines the generator start-up or shutdown status at the time t, based on its 0/1 status between hours $t-1$ and t. $y_{i,t}$ is the generator start-up status and $z_{i,t}$ is the generator shut down status. Constraint (3) restricts the generator to start up and shut down within the same time interval.

$$\sum_{j\in J} q_{i,t,j} = y_{i,t}, \quad \forall t \in T, i \in I \quad (4)$$

$$su_{i,t} = \sum_{j\in J} SUC_{i,j}.\, q_{i,t,j}, \quad \forall t \in T, i \in I \quad (5)$$

Constraint (4) & (5) determines the exact points of the start-up curve at which generator has not been in service. The start-up cost of each generator depends on the service hours. Here $q_{i,t,j}$ is the generator start-up cost identification matrix and $SUC_{i,j}$ is the cost of segment j. Constraint (6) determines the exact points of the start-up curve at which generator has not been in service.

$$g_{i,t,n} = \sum_{b\in B} g_{i,t,b,\mathrm{n}}^{seg}, \quad \forall t \in T, i \in I, n \in N \quad (6)$$

$$\underline{G}_i.x_{i,t} \le g_{i,t,n} \le \overline{G}_i.x_{i,t}, \quad \forall t \in T, i \in I, n \in N \quad (7)$$

$$-\underline{R}_i \le g_{i,t,n} - g_{i,t-1,n} \le \overline{R}_i, \quad \forall t \in T, i \in I \quad (8)$$

Power output of individual generators is taken as the sum of the output on each part of its cost curve, as defined by constraint (7). Here, $\overline{G}_i$ and $\underline{G}_i$ denotes maximum and minimum power output of the generator. Constraint (8) sets the up and down ramp limits for each scenario, $\overline{R}_i$ and $\underline{R}_i$ are ramp up and ramp down limit of generator.

PFR constraints (9) – (17) aims to control the initial deviation of frequency within prescribed limit, following a maximum infeed loss. Constraint (9) ensures that enough inertial response should be available so that the maximum RoCoF does not trigger protective relays like UFLS relay or cause instability. Here H_i is the inertia constant of

generator i, $H^{eq}_{L_{inertia}}$ is equivalent load inertia (s), H_{req} is the required inertia (s), $P^{d}_{t,b}$ is the load at bus b during t. Constraint (10) ensures PFR adequacy, $P_{f_{i,t}}$ is the variable for total PFR availability (MW), P^{C}_{R} is the constant for PFR capacity requirement (MW), ε is the load damping rate (1/Hz) and $\Delta f^{\max}$ is the maximum frequency deviation (Hz). Constraint (11) generates the equivalent droop curve R^{dre}, represented as Hz/MW. Eqn. (12) ensure that adequate headroom is available with enabling of governor for providing PFR and maintaining the droop curve relationship. Constraint (13) requires the generator to be online when its governor is enabled. Constraint (14) disables the generators by assigning x equal to 0, which are working in the mode that couldn't provide PFR, while constraint (15) sets δ equal to 0 for the generators having large governor dead-band.

$$\sum_{i\in I}\left\{x_{i,t} * H_i * \overline{G}\right\} + H^{eq}_{L_{inertia}} * D_{t,s} \geq H_{req} - R^{ins}_{t,inertia} \forall t \in T \tag{9}$$

$$\sum_{i\in I} P_{f_{i,t}} \geq P^{C}_{R} - \varepsilon * P^{d}_{t,b} * \frac{\Delta f^{\max}}{f_0} - R^{ins}_{t,P_f}, \quad \forall t \in T \tag{10}$$

$$R^{dre}_{i} = \frac{R^{drc}_{i} * f_0}{\overline{G}_i}, \qquad \forall i \in I \tag{11}$$

$$P_{f_{i,t}} \leq \frac{\delta_{i,t}}{R^{dre}_{i}}(\Delta f^{\max} - G^{db}_{i}), \quad \forall i \in I, \forall t \in T \tag{12}$$

$$P_{f_{i,t}} \geq \frac{\Upsilon_{i,t}}{R^{dre}_{i}}(\Delta f^{\max} - G^{db}_{i}) - \overline{G}_i(1-\delta_{i,t}), \forall i \in I, \forall t \in T \tag{13}$$

$$\delta_{i,t} \leq x_{i,t} \forall i \in I, \quad \forall t \in T \tag{14}$$

$$\delta_{i,t} = 0 \quad \forall i \in G_{ng}, \quad \forall t \in T \tag{15}$$

Eqn. (16) and (17) checks the requirements of PFR and ensures that adequate PFR is available at nadir time, t^{nadir} and intermediate steady-state time, t^{ss}.

$$\sum_{i\in I} P_{f_{i,t}} \geq P^{req}_{ss_{i,t}} - P^{C}_{R\ ss} \quad \forall t \in T \tag{16}$$

$$\sum_{i\in I} P_{nadir_{i,t}} \geq P^{req}_{nadir_{i,t}} - P^{C}_{R\ nadir} \quad \forall t \in T \tag{17}$$

IV. Wind & PV Uncertainty Characterization

For uncertainty modeling using ARIMA model, first the degree of differentiation and order of suitable ARIMA model is determined on the basis of collected historical data. The degree of differentiation is determined by the differentiation of non-stationary sample historical wind and PV power time series until it becomes a stationary time series. Order of AR and MA terms are obtained by the observation of ACF and PACF plot of differentiated wind & PV power time series. The typical ARIMA (p, d, q) model is expressed as

$$\alpha_p(\beta)(1-\beta)^d \lambda_t = \psi_0 + \psi_q(\beta)\zeta_t \tag{18}$$

where λ_t is the prediction limit of wind & PV power at time interval t, d is the degree of differentiation, β is the backshift operator, $\alpha_p(\beta)$ is the AR operator of order p, and $\psi_q(\beta)$ is the MA operator of order q. ζ_t is a random number distributed normally with zero mean and constant variance. This is also known as white noise or error signal. For simplicity, modeling of seasonal weather impacts on the wind power uncertainty is not considered.

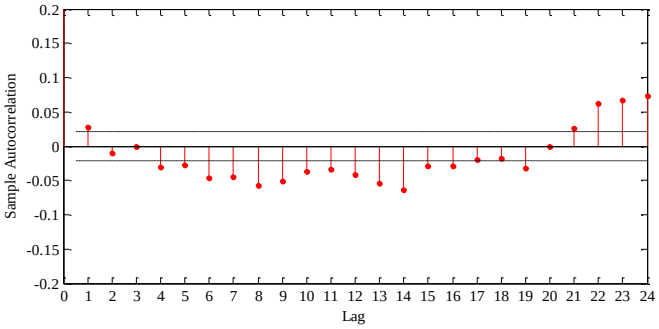

Fig. 2 ACF plot of sample wind power data.

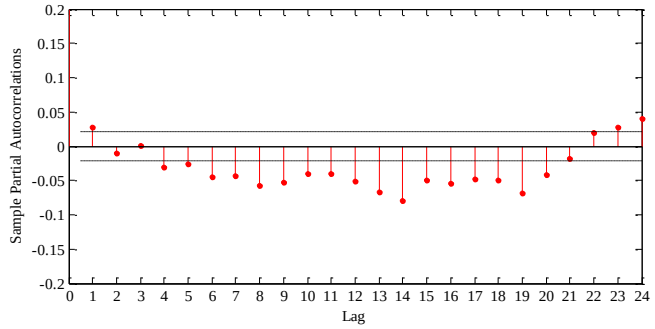

Fig. 3 PACF plot of sample wind power data.

From Figs. 2 & 3, it is clearly visualized that ACF as well as PACF are cutoff after first lag for wind. Therefore, the ARIMA (1,1,1) model is suitable for forecasting intervals and generating scenarios of sample wind power time series. The estimated values of AR and MA coefficients are 0.619 and 0.614. The estimated value of white noise variance is 0.983. For PV generation ARIMA (3, 0, 0) model is found suitable for generating scenarios of sample PV power time series as observed from ACF & PACF plot of Figs. 6 & 7. The estimated values of AR1, AR2 and AR3 are 1.820, -1.031 and 0.383 while values of variance are 0.236. Wind speed historical time series data for the duration 01.01.2010 to 31.12.2010 is used, online available from Illinois Institute of Rural Affair, USA [12]. Solar radiation data of one year from 01.01.2010 to 31.12.2010 from Chicago, USA is used in this study [13]. Wind & PV power uncertainty is modelled in SUC model by considering 1000 wind power scenario generations. After scenario generation, backward reduction algorithm is utilized to obtain 10 representative scenarios. It is observed that both generated and reduced scenarios vary around their mean value, with 95% confidence interval. Reduced wind power scenarios are used in SUC model for modeling wind

and PV power uncertainty. The generated & reduced scenarios of wind & PV are shown in Fig. 4, 5 & 8, 9 respectively.

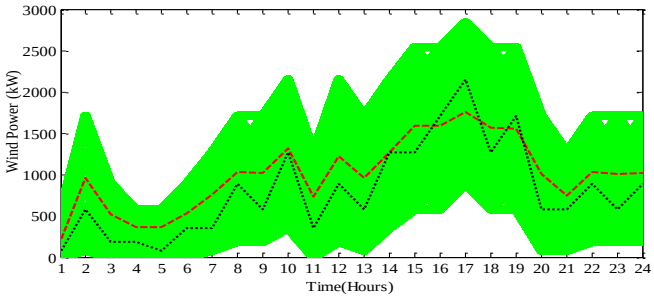

Fig.4. Generated wind power scenarios (green-solid) along with mean scenario (red-dash) and forecasted wind power (black-dotted).

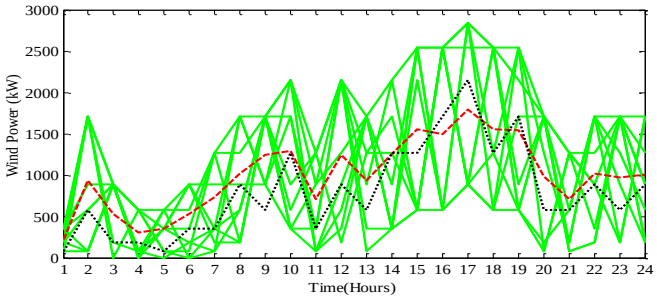

Fig.5. Reduced wind power scenarios (green-solid) along with mean scenario (red-dashed) and forecasted wind power (black-dot).

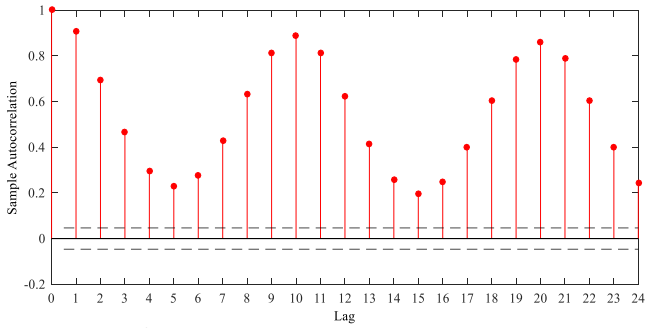

Fig.6. ACF plot of sample PV power data.

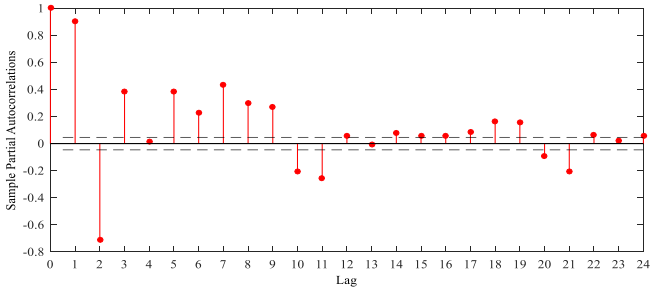

Fig.7. PACF plot of sample PV power data.

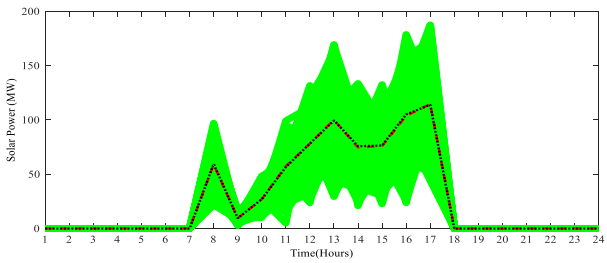

Fig.8. Generated PV power scenarios (green-solid) along with mean scenario (red-dash) and forecasted wind power (black-dotted).

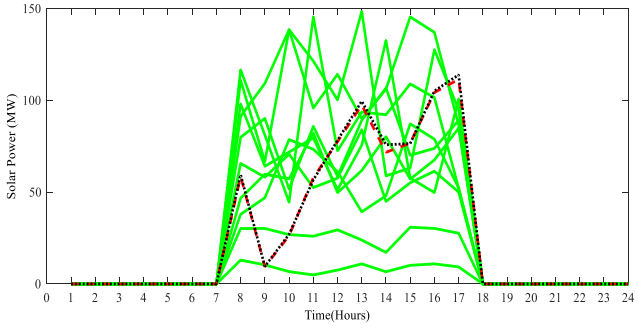

Fig.9. Reduced PV power scenarios (green-solid) along with mean scenario (red-dashed) and forecasted wind power (black-dot).

V. CASE STUDY

One area IEEE reliability test system [14], is used to implement the PFR constrained stochastic UC. There are 24 buses, including 17 load buses and 32 generators. The generation mix includes eleven oil/steam turbine units, nine coal/steam turbine units, six hydro turbine units, four oil/combustion units and two nuclear units. The total installed capacity of generators in one area is 3405 MW with peak load 2850 MW. The data is modified to include 700 MW generation from wind plant and 422 MW from PV plant. The penetration level is varied in 10 to 30% range. Nominal frequency (=50 Hz), governor droop (= 5%), frequency dead band (=15 mHz), load damping rate (=1%/Hz) , RoCoF of 0.5Hz/s and delivery time (=10 s) are chosen according to National Grid standards [15]. The largest generators in the system are two nuclear units of 400 MW, and infeed loss of one of the unit is considered. PFR capacity of system should limit frequency above minimum value of 49.2 Hz. The maximum requirement is assumed to be 30% of the total responsive capacity and for all the governors should at least be greater than 100 mHz. is assumed to be 10000 $/MW-h. Generator frequency response parameters are mentioned in Table I. This characterization represents different generation types, thus avoiding the need to adopt separate model for different generation types.

TABLE I
GENERATOR FREQUENCY RESPONSE PARAMETERS [25]

Unit	G_i^{up} (MW)	H_i (s)	R^{drc} (p.u.)	G^{db} (mHz)
U12	12	2.6	0.05	15
U20	20	2.8	0.05	15
U50	50	3.5	0.05	15
U76	76	3.0	0.05	15
U100	100	2.8	0.05	15
U155	155	3.0	0.05	15
U197	197	2.8	0.05	15
U350	350	3.0	0.05	15
U400	400	5.0	0.05	15

A. PFR schedules with Cost Performance

This section details the performance of frequency response parameter, considering largest generation outage. The response provided by each unit is shown in Table I. Figs. 4 and 5 show the operation and PFR cost with increased PV penetration level. Addition of PFR constraints reduces the average units committed online per hour. PFR constraints add only about 0.2% in total operation cost, which is not substantially higher than the considered duality gap of MILP solver (0.1%). This is because of the

committed inertial and PFR response of the system. Here, synchronous inertial cost is assumed zero for all hours, as the system has sufficient committed inertial and PFR response.

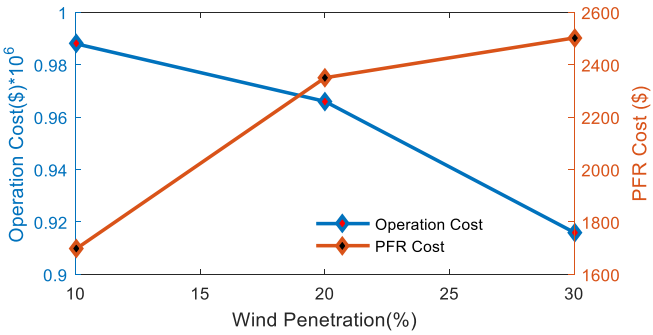

Fig. 10. Operation cost and PFR cost with varying wind and PV penetration.

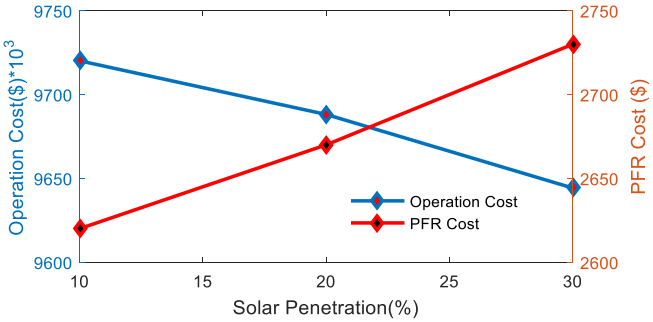

Fig. 11. Operation cost and PFR cost with varying wind and PV penetration.

TABLE I GENERATOR PFR SCHEDULES

	DUC	*SUC*
PFR (MW): U-12	2	3.2
PFR (MW): U-20	4	5.4
PFR (MW): U-76	11	20.3
PFR (MW): U-100	17	27.72
PFR (MW): U-197	19	55.28
PFR (MW): U-350	28	68.45
PFR (MW): U-350	28	19.4

VI. CONCLUSION

This paper presents a novel SUC model for optimizing PFR schedules in the light of wind and PV uncertainty at different penetration levels. ARIMA model is used for the scenario generation of wind & PV power time series, backward reduction algorithm is used to reduce these scenarios to obtain the representative scenarios required in SUC model for the wind and PV power uncertainty modelling. Case studies are performed to compare the proposed method with conventional DUC model in terms of operation and PFR cost, PFR adequacy. Numerical results show that the SUC model with PFR constraints is an effective way of handling wind & PV uncertainty with overall cost reduction and optimized PFR schedules. The solution obtained has the potential to provide information for enhanced frequency control capability in future low carbon power system.

REFERENCES

[1] Global Wind Statistics-2016 [online]. Available: http://www.gwec.net/wp-content/uploads/.

[2] Global Solar Forecast – A brighter outlook for global PV installations [online]. Available: http://www.mercomcapital.com/global-solar-forecast-a-brighter-outlook-for-global pv installations.

[3] S. Sharma, S. Huang, and N. Sarma, "System inertial frequency response estimation and impact of renewable resources in ERCOT interconnection," *IEEE PES GM*, San Diego, July 2011.

[4] R. Doherty et al., "An assessment of the impact of wind generation on system frequency control," *IEEE Trans. Power Syst.*, vol. 25, no. 1, pp. 452–60, Jan. 2010.

[5] M. Dreidy, H. Mokhlis, S. Mekhilef, "Inertia response and frequency control techniques for renewable energy sources: A review," *Renew. Sust. Ener. Reviews*, pp. 144-155, Nov. 2016.

[6] System operability framework, 2015, [online]. Available: http://www2.nationalgrid.com/UK/Industry-information/ Future-of-Energy/ System-Operability-Framework/.

[7] J. F. Restrepo and F. Galiana, "Unit commitment with primary frequency regulation constraints," IEEE Trans. Power Syst., vol. 20, no. 4, pp. 1588–1596, Nov. 2005.

[8] H. Ahmadi and H. Ghasemi, "Security-constrained unit commitment with linearized system frequency limit constraints," *IEEE Trans. Power Syst.*, vol. 29, no. 4, pp. 1536–1545, July 2014.

[9] F. Teng, V. Trovato, and G. Strbac, "Stochastic scheduling with inertia-dependent fast frequency response requirements," *IEEE Trans. Power Syst.*, vol. 31, no. 2, pp. 1557–1566, Mar. 2016.

[10] Frequency Response Standard White paper prepared by the Frequency Task Force of the NERC Resources Subcommittee, 2004.

[11] H. Pandzic, Y. Dvorkin, T. Qiu, Y. Wang, and D. S. Kirschen, "Toward cost-efficient and reliable unit commitment under uncertainty," IEEE Trans. Power Syst., vol. 31, no. 2, pp. 970–982, Mar. 2016.

[12] "U.S. Energy Information Administration. 'Short-Term Energy Outlook," [Online].Available: http://www.eia.gov/forecasts/steo.

[13] SolarAnywhere[Online].Avaiable:https://data.solaranywhere.com/Public/ Tutorial.aspx.

[14] Reliability Test System Task Force, "The IEEE reliability test system—1996," IEEE Trans. Power Syst., vol. 14, no. 3, pp. 1010–1020, Aug. 1999.

[15] National Grid, Security and Quality of Supply Standards [Online]. Available: http://www2.nationalgrid.com/UK/Industry-information/Electricity-codes/System-Security-and-Quality-of-Supply-Standards/.